**ONCOLOGY**

CrossMark

# 68Ga-PSMA-PET/CT in comparison with 18F-fluoride-PET/CT and whole-body MRI for the detection of bone metastases in patients with prostate cancer: a prospective diagnostic accuracy study

Eva Dyrberg[1,2] • Helle W. Hendel[2] • Tri Hien Viet Huynh[2] • Tobias Wirenfeldt Klausen[3] • Vibeke B. Løgager[1] • Claus Madsen[2] • Erik M. Pedersen[4] • Maria Pedersen[2] • Henrik S. Thomsen[1]

## Abstract

**Objectives** To determine the diagnostic accuracy of $^{68}$gallium prostate-specific membrane antigen (PSMA)-based positron emission tomography/computed tomography (PET/CT) in comparison with $^{18}$F-fluoride-based PET/CT (NaF-PET/CT) and whole-body magnetic resonance imaging (WB-MRI) for the detection of bone metastases in patients with prostate cancer.

**Methods** Sixty patients with prostate cancer were included in the period May 2016 to June 2017. The participants underwent three scans (index tests) within 30 days: a NaF-PET/CT, a WB-MRI and a PSMA-PET/CT. Experienced specialists assessed the scans. In the absence of a histological reference standard, the final diagnosis was determined as a panel diagnosis. Measures of the diagnostic performances of the index tests were calculated from patient-based dichotomous outcomes (0 or $\geq 1$ bone metastasis) and pairwise compared (McNemar test). For each index test, the agreement with the final diagnosis with regard to the number of bone metastases detected (0, 1–5, > 5) and the inter-reader agreement was calculated (kappa coefficients).

**Results** Fifty-five patients constituted the final study population; 20 patients (36%) were classified as having bone metastatic disease as their final diagnosis. The patient-based diagnostic performances were (sensitivity, specificity, overall accuracy) PSMA-PET/CT (100%, 100%, 100%), NaF-PET/CT (95%, 97%, 96%) and WB-MRI (80%, 83%, 82%). The overall accuracy of PSMA-PET/CT was significantly more favourable compared to WB-MRI ($p = 0.004$), but not to NaF-PET/CT ($p = 0.48$). PSMA-PET/CT classified the number of bone metastases reliably compared to the final diagnosis (kappa coefficient 0.97) and with an "almost perfect" inter-reader agreement (kappa coefficient 0.93).

**Conclusions** The overall accuracy of PSMA-PET/CT was significantly more advantageous compared to WB-MRI, but not to NaF-PET/CT.

### Key Points
• *PSMA-PET/CT assessed the presence of bone metastases correctly in all 55 patients*
• *PSMA-PET/CT was more advantageous compared to WB-MRI*
• *No difference was found between PSMA-PET/CT and NaF-PET/CT*

**Keywords** Positron emission tomography computed tomography · Magnetic resonance imaging · Prostatic neoplasms · Metastasis · Bone and bones

✉ Eva Dyrberg
edyrberg@hotmail.com

[1] Department of Radiology, Copenhagen University Hospital Herlev and Gentofte, Herlev Ringvej 75, DK-2730 Herlev, Denmark

[2] Department of Clinical Physiology and Nuclear Medicine, PET and Cyclotron, Copenhagen University Hospital Herlev and Gentofte, DK-2730 Herlev, Denmark

[3] Department of Hematology, Copenhagen University Hospital Herlev and Gentofte, DK-2730 Herlev, Denmark

[4] Department of Radiology, Aarhus University Hospital, DK-8000 Aarhus C, Denmark

🢡 Springer

**Abbreviations**

| | |
|---|---|
| ADC | Apparent diffusion coefficient |
| ADT | Androgen deprivation therapy |
| BVC | Best valuable comparator |
| CT | Computed tomography |
| DWI | Diffusion-weighted images |
| eGFR | Estimated glomerular filtration rate |
| HBED-CC | $N,N'$-bis[2-hydroxy-5-(carboxyethyl) benzyl]ethylenediamine-$N,N'$-diacetic acid |
| MRI | Magnetic resonance imaging |
| NaF | Sodium fluoride |
| PET | Positron emission tomography |
| PSA | Prostate-specific antigen |
| PSMA | Prostate-specific membrane antigen |
| SPECT | Single-photon emission computed tomography |
| STARD | Standards for Reporting of Diagnostic Accuracy Studies |
| STIR | Short-T1 inversion recovery |
| T1w | T1-weighted |
| WB | Whole-body |
| 95%CI | 95% confidence interval |
| $^{18}$F | Fluoride-18 |
| $^{68}$Ga | Gallium-68 |
| $^{68}$Ge | Germanium-68 |
| $^{177}$Lu | Lutetium-177 |

## Introduction

In patients with prostate cancer the skeleton is the most frequent site of metastatic disease, and bone metastases are present in approximately 80% of the patients with advanced disease [1]. Prostate cancer cells metastasise from the prostate gland via a haematogenous or lymphatic route to the well-vascularised red bone marrow [1, 2]. In the bone marrow, the tumour cells interact with the cellular components of the bone marrow microenvironment and the bone matrix (osteoblasts and osteoclasts) leading to an osseous response [3]. This response is dominated by a reactive bone formation caused by a relative excess of osteoblast activity resulting in osteoblastic (osteosclerotic) bone metastases [2, 4, 5]. Thus, bone marrow metastases precede the involvement of the bone cortex and the osteoblastic bone metastases [5, 6].

An accurate detection of the presence of bone metastases is important throughout the disease course of prostate cancer to select an optimal treatment strategy and to reduce potential complications [2]. With the continuous development of novel imaging techniques, the clinicians' choice of imaging modality is probably more complex than ever. Conventional bone scintigraphy has been considered the international reference standard for several decades and is included in the international guidelines for management of prostate cancer [7, 8]. However, the more novel imaging methods positron emission tomography–computed tomography (PET/CT) and whole-body magnetic resonance imaging (WB-MRI) have been suggested to offer diagnostic advantages [9, 10].

$^{68}$Ga prostate-specific membrane antigen ($^{68}$Ga-PSMA) is a new cancer-targeting PET tracer that accumulates corresponding to prostate cancer tumour cells [11]. The $^{68}$Ga-labelled PSMA ligand is extracted from a $^{68}$Ge/$^{68}$Ga radionuclide generator, and several PSMA ligands are currently in use with PSMA-11 (PSMA-HBED-CC) being the most common [12, 13]. PSMA is a membrane-bound enzyme that is overexpressed in prostate cancer cells within the prostate gland, lymph nodes, soft tissue and bones. The radiolabelled PSMA binds as a ligand to the extracellular domain of PSMA and is subsequently internalised [14]. Preliminary results of the diagnostic performance of $^{68}$Ga-PSMA-PET/CT are promising [15, 16]. However, surprisingly few prospective diagnostic accuracy studies have aimed to elucidate the role of PSMA-PET/CT in the detection of bone metastases in patients with prostate cancer.

The imaging modalities $^{18}$F-fluoride-based PET/CT (NaF-PET/CT) and WB-MRI have been shown to detect bone metastases with a high accuracy [17, 18]. NaF-PET/CT visualises the osteoblastic bone response to the presence of tumour cells in the bone marrow. Conventional MRI sequences depict tumour cells that have replaced the bone marrow, and diffusion-weighted MRI sequences (DWI) depict the restricted water diffusion caused by the tumour cells [19, 20].

To the best of our knowledge, no previous prospective study has compared the diagnostic performances of PSMA-PET/CT, NaF-PET/CT and WB-MRI. Therefore, the aim was to perform a diagnostic accuracy study on the detection of bone metastases by means of PSMA-PET/CT in comparison with NaF-PET/CT and WB-MRI in patients with prostate cancer.

## Materials and methods

This is a prospective single-centre study. The regional ethics committee approved the study protocol (approval number H-1-2014-018). Sixty patients gave written informed consent to participate in the period from May 2016 to June 2017.

## Study population

The inclusion criterion was patients with biopsy-proven prostate cancer referred by the clinicians for the standard bone imaging method at our institution, NaF-PET/CT. The patients referred for NaF-PET/CT represented a broad disease spectrum from newly diagnosed to patients with known bone metastases. Exclusion criteria were patients receiving chemotherapy or abiraterone treatment, prior radiotherapy of bone metastases, prior malignancy (except for adequately treated basal cell or squamous cell skin cancer), bone metabolism

disorder, osteomyelitis and any conditions contraindicated for MRI scan or a CT contrast agent.

The patients were consecutively invited to participate immediately after the routine NaF-PET/CT. Each patient was only allowed to enter the study once during the inclusion period. Patients willing to participate underwent three scans within 30 days: a routine NaF-PET/CT, a PSMA-PET/CT and a whole-body MRI.

Five patients were excluded from the subsequent analyses as a result of an incomplete/lacking scan, change in therapy between the three scans and an insufficient image acquisition due to technical scanner problems. A flow diagram of patient inclusion is shown in Fig. 1.

## Reporting

Reporting was done in accordance with the Standards for Reporting of Diagnostic Accuracy Studies (STARD) statement [21]. In accordance with the STARD definition, the three imaging techniques (PSMA-PET/CT, NaF-PET/CT, WB-MRI) whose accuracies were evaluated are referred to as "index tests".

## Imaging protocols

The routine NaF-PET/CT scan was performed with Biograph mCT (Siemens Healthineers). Images were obtained from the top of the skull to just below the knees. The table time was approximately 10 mins.

The PSMA-PET/CT scan was performed with Biograph mCT (Siemens Healthineers). Images were obtained from the top of the skull to just below the knees. The table time was approximately 30 mins.
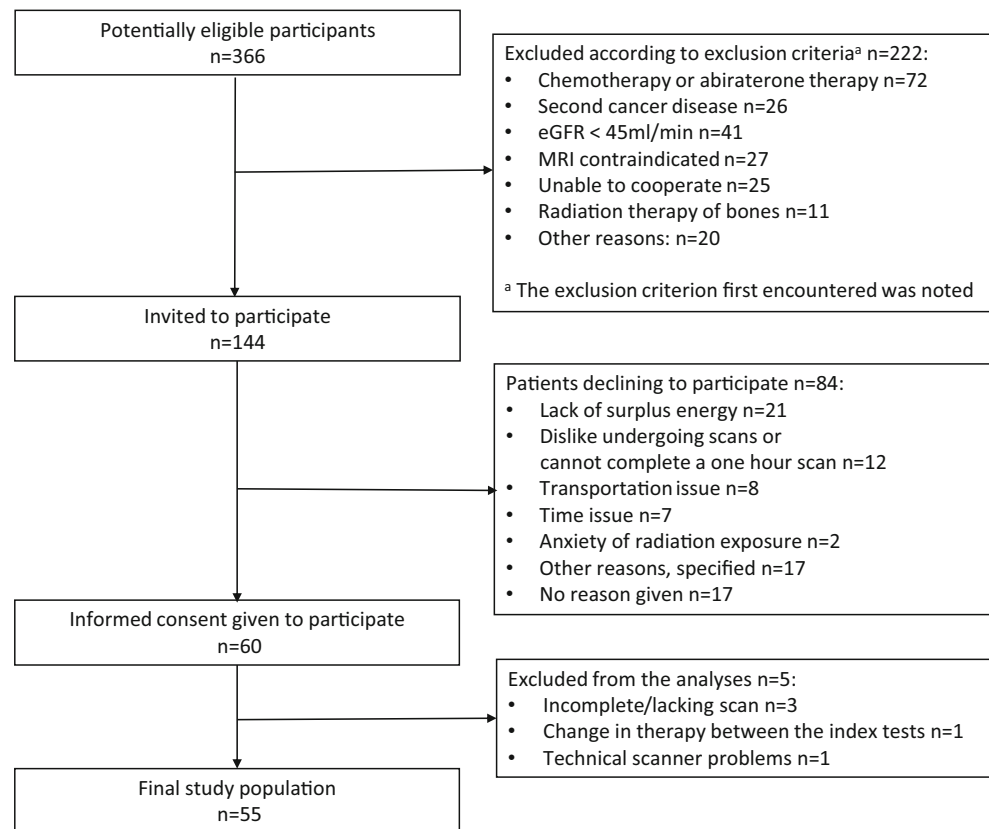
WB-MRI was performed with whole-body 3.0-T Ingenia (Philips Healthcare). Images were obtained from the top of the skull to the feet. The examination protocol consisted of coronal T1-weighted (T1w), sagittal T1w of the vertebral spine, coronal STIR-weighted and axial DWI (b0, b1000). The total scan time was approximately 70 mins.

Further technical scanner details are presented in Appendix E1 and E2.

## Imaging analysis

The image analysis was performed visually at a workstation and blinded to other imaging results and clinical data except the fact that the patients were known to suffer from prostate cancer and were referred for a routine NaF-PET/CT. All images were read anonymised and separately by two specialists with 8–21 years of experience: two nuclear medicine specialists read PSMA-PET/CT and NaF-PET/CT (HWH, CM), and two radiologists read WB-MRI (VBL, EMP). The readings were performed after the inclusion of the last participant and

Fig. 1 Flow diagram illustrating the inclusion of study participants



**Potentially eligible participants**
n=366

**Excluded according to exclusion criteria[a] n=222:**
- Chemotherapy or abiraterone therapy n=72
- Second cancer disease n=26
- eGFR < 45ml/min n=41
- MRI contraindicated n=27
- Unable to cooperate n=25
- Radiation therapy of bones n=11
- Other reasons: n=20

[a] The exclusion criterion first encountered was noted

**Invited to participate**
n=144

**Patients declining to participate n=84:**
- Lack of surplus energy n=21
- Dislike undergoing scans or cannot complete a one hour scan n=12
- Transportation issue n=8
- Time issue n=7
- Anxiety of radiation exposure n=2
- Other reasons, specified n=17
- No reason given n=17

**Informed consent given to participate**
n=60

**Excluded from the analyses n=5:**
- Incomplete/lacking scan n=3
- Change in therapy between the index tests n=1
- Technical scanner problems n=1

**Final study population**
n=55

within a short period of time. The readers of the two PET/CT scans had a period of minimum 1 month between readings on the same patient to eliminate recall bias. Each reader assessed whether 0, 1–5 or > 5 bone metastases were present. In patients with 1–5 bone metastases the exact number and anatomical localisation were noted. Discrepancies between the two readers were solved at a consensus meeting.

On NaF-PET/CT and PSMA-PET/CT, the patient was diagnosed with bone metastases if the intensity and the pattern of the tracer accumulation were considered highly suspicious of metastatic bone disease with or without corresponding findings on the CT scan (focal uptake significantly above background level and not considered benign).

On MRI bone metastases were diagnosed corresponding to lesions with hypointense signal intensity on T1w, intermediate or high signal intensity on STIR, and high signal intensity on DWI b1000 combined with low signal intensity on ADC. No quantitative cut-off value was applied for ADC. MRI lesions smaller than 5 mm were not characterised, as recommended in the literature [3].

## Final diagnosis

In the absence of a histological reference standard, the final diagnosis (0, 1–5, > 5 bone metastases) was determined as a panel diagnosis by three imaging specialists (HWH, CM, VBL) with several years of experience from weekly multidisciplinary conferences on patients with prostate cancer. The panel meeting took place half a year after the inclusion of the last study participant.

In patients with a concordant diagnosis of the three index tests regarding the number of bone metastases (i.e. all three methods detected either 0, 1–5 or > 5 bone metastases), this diagnosis was considered the final diagnosis. In patients with a discordant diagnosis of the three index tests, the panel determined the final diagnosis on the basis of a review of clinical data from patient files (clinical, medical, laboratory and pathological files) and a side-by-side evaluation of the index tests and available clinical follow-up images (including NaF-PET/ CT, MRI and CT scans). The plenary decision process was validated in a comparable previous study. The follow-up period ranged from 0.5 to 1.5 years. A summary of how the final diagnoses were established is presented in Appendix E3.

## Statistical analysis

The data analyses were performed using R software (version 3.2.3; www.r-project.org). 

Measures of the diagnostic performances of the index tests were calculated from patient-based dichotomous outcomes (0 or ≥ 1 bone metastasis). A Cochran's $Q$ test was performed

to compare the diagnostic performances (sensitivity, specificity, overall accuracy) of the three imaging methods, and McNemar test was performed for pairwise comparisons. The agreement between each index test and the final diagnosis with regard to the number of detected bone metastases (0, 1–5, > 5) was assessed with calculated kappa coefficients. To investigate whether the index tests had a tendency to over- or underestimate the number of bone metastases, a Wilcoxon signed rank test was performed. Inter-reader variability was determined calculating kappa coefficients.

A $p$ value less than 0.05 was considered statistically significant. $P$ values for pairwise comparisons are shown unadjusted, but information on adjustments using the Bonferroni–Holm method is presented.

# Results

## Final study population

Fifty-five patients (aged 54–91 years) constituted the final study population and were referred for a routine NaF-PET/CT for the following reasons: initial staging based on risk profile ($n = 10$), suspicion of progression in patients in active surveillance ($n = 3$) or watchful waiting ($n = 5$) and monitoring of patients in androgen deprivation therapy (ADT) ($n = 37$) (Table 1).

On average 10 days elapsed between the routine NaF-PET/ CT and the WB-MRI (range 2–28 days) and the PSMA-PET/CT (range 1–27 days), respectively.

## Inter-reader agreement

A discrepancy in the number of bone metastases (0, 1–5, > 5) assessed by two readers (necessitating a consensus meeting) was observed in the following proportion of patients: 4% (2/55) for PSMA-PET/CT, 4% (2/55) for NaF-PET/CT and 18% (10/55) for WB-MRI. Determination of inter-reader variability resulted in kappa values corresponding to "almost perfect" agreement (PSMA-PET/CT, NaF-PET/CT) and "substantial" agreement (WB-MRI) (Appendix E4).

## Final classification of metastatic bone disease

Twenty out of the 55 patients (36%) were classified as having metastatic bone disease as their final diagnosis: nine patients with 1–5 bone metastases and 11 with > 5 bone metastases. Seven out of 11 patients classified with > 5 bone metastases had countable isolated lesions, whereas the remaining four patients had unidentifiable lesions due to regional ($n = 3$) or global diffuse disease ($n = 1$).

The baseline characteristics of the patients classified with and without bone metastatic disease respectively are presented in Table 1.

**Table 1** Characteristics of study participants

| Parameter | All (n = 55) | Bone metastatic disease (n = 20) | No bone metastatic disease (n = 35) |
|---|---|---|---|
| At time of diagnosis | | | |
|   Mean PSA (ng/mL) | 87 (range 5–1000) | 138 (range 6–1000) | 58 (range 5–479) |
|   Median PSA (ng/mL) | 30 (IQR 11–72) | 44 (IQR 13–178) | 25 (IQR 9–50) |
| Gleason grade groups[a] | | | |
|   Gleason grade group 1 (Gleason score 3 + 3) | 6 (11%) | 0 (0%) | 6 (17%) |
|   Gleason grade group 2 (Gleason score 3 + 4) | 6 (11%) | 1 (5%) | 5 (14%) |
|   Gleason grade group 3 (Gleason score 4 + 3) | 13 (24%) | 5 (25%) | 8 (23%) |
|   Gleason grade group 4 (Gleason score 4 + 4, 3 + 5, 5 + 3) | 14 (25%) | 6 (30%) | 8 (23%) |
|   Gleason grade group 5 (Gleason score 4 + 5, 5 + 4, 5 + 5) | 14 (25%) | 6 (30%) | 8 (23%) |
|   NA | 2 (4%) | 2 (10%) | 0 (0%) |
| D'Amico risk classification | | | |
|   Low risk | 1 (2%) | 0 (0%) | 1 (3%) |
|   Intermediate risk | 8 (15%) | 1 (5%) | 7 (20%) |
|   High risk | 28 (51%) | 11 (55%) | 17 (49%) |
|   NA[b] | 18 (33%) | 8 (40%) | 10 (29%) |
| At time of study inclusion | | | |
|   Mean age in years | 75 (SD 9, range 54–91) | 75 (SD 9, range 54–91) | 74 (SD 8, range 59–91) |
|   Mean years with prostate cancer | 4 (SD 4, range 0–17) | 4 (SD 4, range 0–17) | 4 (SD 3, range 0–12) |
| Reason for referral | | | |
|   Initial staging based on risk profile | 10 (18%) | 3 (15%) | 7 (20%) |
|   Active surveillance, progression suspicion | 3 (5%) | 0 (0%) | 3 (9%) |
|   Watchful waiting, progression suspicion | 5 (9%) | 1 (5%) | 4 (11%) |
|   Monitoring of androgen deprivation therapy (ADT)[c] | 37 (67%) | 16 (80%) | 21 (60%) |
|   Patients with castration-resistant prostate cancer (CRPC) | 20 (36%) | 12 (60%) | 8 (23%) |

Unless otherwise indicated, data are numbers of patients

*NA* not available, *PSA* prostate-specific antigen, *FD* final diagnosis, *IQR* interquartile range

[a] International Society of Urological Pathology (ISUP) 2014 Gleason grade groups [22]

[b] Most frequently not available because of lack of clinical T stage

[c] ADT includes prior orchiectomy, treatment with antiandrogens or inhibitors of gonadal androgen synthesis

## Patient-based diagnostic accuracy measurements

PSMA-PET/CT correctly classified all patients, NaF-PET/CT misclassified two patients (false positive n = 1, false negative n = 1) and WB-MRI misclassified 10 patients (false positive n = 6, false negative n = 4) (Table 2).

The patient misclassified as false positive on NaF-PET/CT was diagnosed with a solitary bone metastasis in the pelvis.

**Table 2** Patient-based diagnostic performances

| | PSMA-PET/CT | NaF-PET/CT | WB-MRI |
|---|---|---|---|
| True positive results | 20 (36%) | 19 (35%) | 16 (29%) |
| False positive results | 0 (0%) | 1 (2%) | 6 (11%) |
| True negative results | 35 (64%) | 34 (62%) | 29 (53%) |
| False negative results | 0 (0%) | 1 (2%) | 4 (7%) |
| Sensitivity % | 100 (CI 83–100) | 95 (CI 75–100) | 80 (CI 56–94) |
| Specificity % | 100 (CI 90–100) | 97 (CI 85–100) | 83 (CI 66–93) |
| Positive predicative value % | 100 (CI 83–100) | 95 (CI 75–100) | 73 (CI 50–89) |
| Negative predicative value % | 100 (CI 90–100) | 97 (CI 85–100) | 88 (CI 72–97) |
| Overall accuracy % | 100 (CI 94–100) | 96 (CI 87–100) | 82 (CI 69–91) |

*CI* 95% confidence interval

Four out of six false positive WB-MRI patients were diagnosed with a solitary bone metastasis in the spine.

Images from a study participant diagnosed with two bone metastases on PSMA-PET/CT but misclassified as false negative on both NaF-PET/CT and WB-MRI are presented in Figs. 2 and 3 (only one lesion is illustrated). A review of the remaining three false negative WB-MRI patients revealed one patient with a masking artefact from a hip replacement, one patient with an unspecific MRI finding, and one patient without a lesion corresponding to the localisation of the true positive bone metastasis. On a patient-based level the diagnostic performances were (sensitivity, specificity, overall accuracy) PSMA-PET/CT (100%, 100%, 100%), NaF-PET/CT (95%, 97%, 96%) and WB-MRI (80%, 83%, 82%) (Table 2).

Pairwise comparisons revealed that the overall accuracy of PSMA-PET/CT was significantly more favourable compared to WB-MRI ($p = 0.004$). In addition, a tendency towards a more favourable specificity of PSMA-PET/CT compared to WB-MRI was shown ($p = 0.04$), but the difference was not significant after adjustments for pairwise comparisons. No significant differences in the diagnostic performances were found between PSMA-PET/CT and NaF-PET/CT (Table 3).

### Assessment of number of bone metastases

The agreement between each index test and the final diagnosis in regard to the classification of the number of bone metastases (none, oligometastatic (1–5), multiple (> 5)) was "almost perfect" for PSMA-PET/CT (kappa coefficient 0.97, 95% CI

0.90–1.00) and "substantial" for both NaF-PET/CT (kappa coefficient 0.79, 95% CI 0.64–0.95) and WB-MRI (kappa coefficient 0.63, 95% CI 0.44–0.83). No tendency to over- or underestimate the number of bone metastases was observed for neither PSMA-PET/CT ($p = 1.00$), NaF-PET/CT ($p = 0.5$) nor WB-MRI ($p = 0.8$).

The agreement of the three index tests with the final diagnosis per study participant is illustrated with colour codes in Fig. 4.

## Discussion

This study aimed to investigate diagnostic imaging of bone metastases in patients with prostate cancer. The novel imaging technique PSMA-PET/CT correctly classified all study participants. To the best of our knowledge, this is the first prospective diagnostic accuracy study to show a significantly more favourable overall accuracy of PSMA-PET/CT compared to WB-MRI, but not to NaF-PET/CT.

Several studies have focused on determining the detection rate of PSMA-PET/CT for relapse lesions in recurrent prostate cancer [23–27]. However, surprisingly few previous studies have aimed to investigate the diagnostic accuracy of PSMA-PET/CT regarding bone metastases, and the results of PSMA-PET/CT in this study are in line with these [28, 29]. Pyka et al reported in a retrospective study on patients with mixed disease stages ($n = 126$), a patient-based sensitivity and specificity of PSMA-PET of 98.7–100% and 88.2–100%, respectively, and
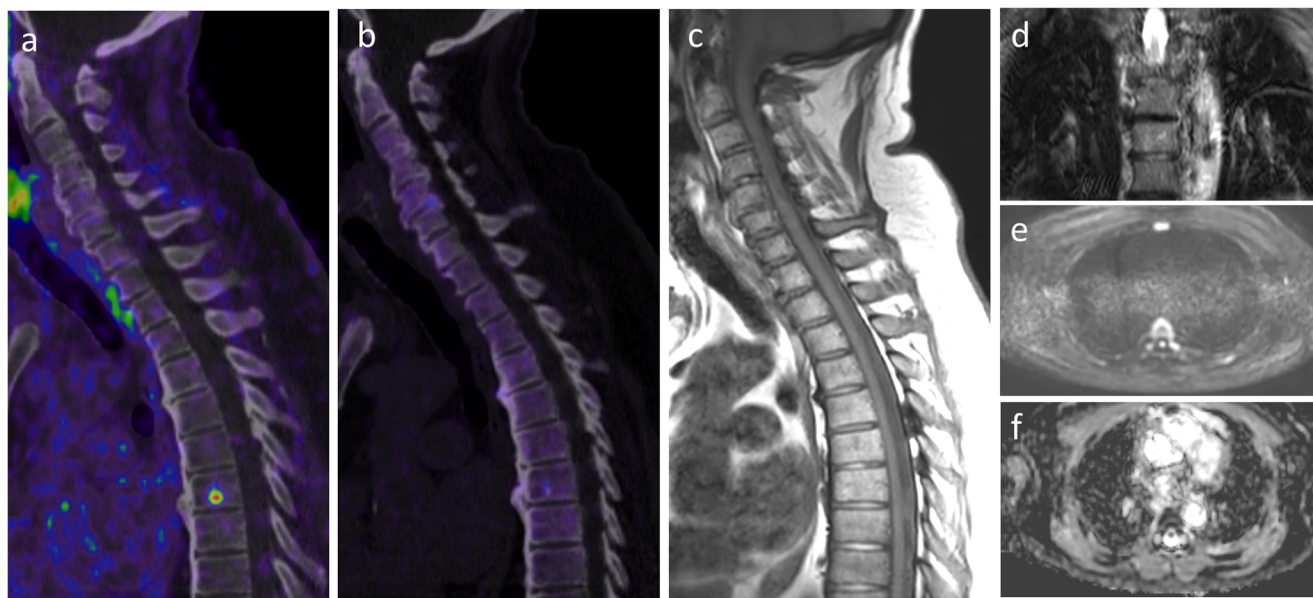


**Fig. 2** Images of a 77-year-old patient with a 4-year history of prostate cancer (Gleason grade group 4, T2c, N1, M0) in androgen deprivation therapy, and referred for bone imaging because of a rising prostate-specific antigen (PSA). (Follow-up images of the same patient are shown in Fig. 3.) PSMA-PET/CT demonstrates focal tracer uptake in the body of Th7 suggestive of a bone metastasis, but no corresponding findings are demonstrated on fluoride-PET/CT and WB-MRI: **a** fused sagittal PSMA-PET/CT, **b** fused sagittal NaF-PET/CT, **c** MRI sagittal T1w, **d** MRI coronal STIR, **e** MRI axial DWI b1000 at the level of T7 and **f** MRI axial ADC at the level of T7

**Fig. 3** Seven months later clinical follow-up images of the same patient as shown in Fig. 2. No change in treatment, but further rise in PSA. NaF-PET/CT now demonstrates findings suspicious of a bone metastasis (focal NaF-uptake in the body of Th7 and corresponding sclerosis has developed on the low-dose CT) confirming the previous diagnosis on PSMA-PET/CT: **a** fused sagittal NaF-PET/CT and **b** sagittal low-dose CT
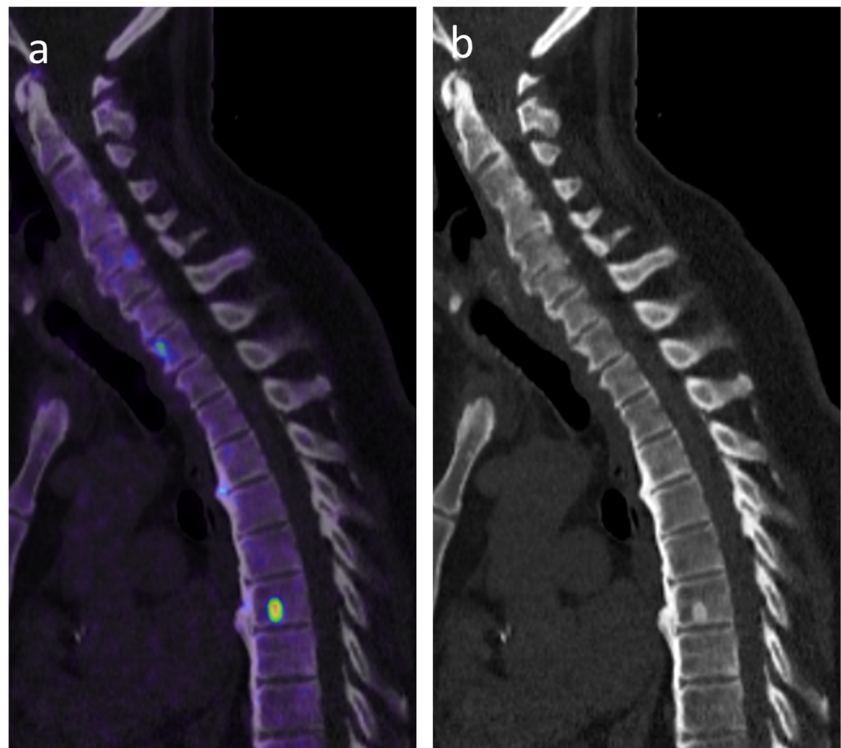


concluded that PSMA-PET outperforms conventional bone scintigraphy [28]. A retrospective study ($n$ = 54) by Janssen et al reported a patient-based sensitivity and specificity of PSMA-PET/CT of 100% and concluded that PSMA-PET/CT outperforms bone SPECT/CT [29]. In both described studies, the final diagnosis was determined by a best valuable comparator (BVC), which is an equivalent to the panel diagnosis applied in this present study.

In line with previous studies, this study reported favourable patient-based diagnostic performances of both NaF-PET/CT and WB-MRI [30–32]. However, WB-MRI had a less favourable overall accuracy compared to both PSMA-PET/CT and NaF-PET/CT, though the latter comparison was not significant after adjustment for pairwise comparisons.

The comparable overall accuracies of PSMA-PET/CT and NaF-PET/CT indicate that the choice between these imaging methods may depend on local parameters like availability, costs and expertise. Institutions with an on-site cyclotron can benefit from the relatively low cost associated with NaF-PET/CT. Furthermore, the throughput of the NaF-PET/CT scanner is relatively high owing to the shorter overall examination time for NaF-PET/CT compared to PSMA-PET/CT. However, at institutions without an on-site cyclotron, the transportation of $^{18}$F-NaF (with a half-life of 110 mins) might not be possible from one centre to another, and the generator-produced $^{68}$Ga-PSMA seems to be a very promising alternative.

For patients with oligometastatic disease, metastases-directed therapies with surgical resection and stereotactic body radiotherapy (SBRT) are becoming an option [33, 34]. In this perspective it is notable that PSMA-PET/CT classified the number of bone metastases (0, 1–5 (oligometastatic) or > 5 (multiple)) "almost perfectly", and thereby seems to be a promising imaging method for stratifying patients to metastases-

**Table 3** Comparison of sensitivity, specificity and overall accuracy

| | Comparison sensitivity | Comparison specificity | Comparison overall accuracy |
|---|---|---|---|
| All three imaging techniques | 0.04[a] | 0.01[a] | 0.0005[a] |
| PSMA-PET/CT vs WB-MRI | 0.13 | 0.04[b] | 0.004 |
| PSMA-PET/CT vs NaF-PET/CT | 1.00 | 1.00 | 0.48 |
| NaF-PET/CT vs WB-MRI | 0.25 | 0.13 | 0.03[b] |

Test results are indicated as $p$ values. McNemar test was performed unless otherwise indicated

[a] Cochran's $Q$ test was performed

[b] $P$ value was not significant after multiple testing adjustments for pairwise comparisons

**Fig. 4** Results of the index tests and the final diagnosis for each study participant represented by a column. Colour codes: green, no metastases; yellow, 1–5 bone metastases; red, > 5 bone metastases
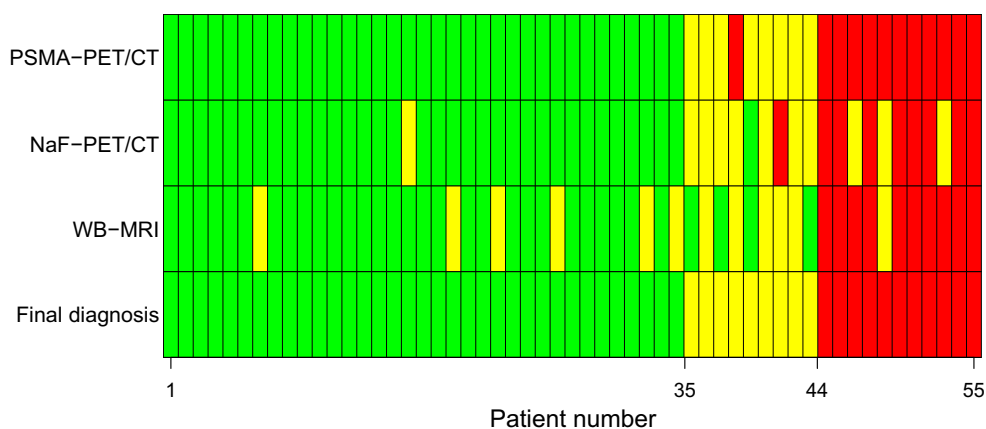


directed therapy. Furthermore, the inter-reader agreement on the PSMA-PET/CT readings was "almost perfect", and this result is in line with the result of a recent larger study [35].

None of the study participants in this study were false positively or false negatively classified with PSMA-PET/CT. However, the name "*prostate-specific* membrane antigen" is misleading, as PSMA is also expressed in a range of normal tissues and in other benign and malignant processes [13, 36]. Furthermore, it has been reported that up to 5% of all prostate cancers do not exhibit a significant PSMA overexpression [37]. Therefore, knowledge of common pitfalls is pivotal for correct interpretation. In this study, a ^{68}Ga-labelled PSMA ligand was investigated. However, a cyclotron requiring ^{18}F labelling of PSMA (^{18}F-PSMA) has recently attracted increased attention [38]. Compared to ^{68}Ga-PSMA, ^{18}F-PSMA can be produced in a larger amount per batch, has a longer half-life and is more suitable for PET imaging because of a better noise reduction [39]. Another promising future perspective is the evolving role of PSMA-PET/CT in the emerging PSMA targeting treatments in advanced prostate cancer (e.g. [177]Lu PSMA therapy) evaluating target expression and treatment response [12, 13, 39].

In clinical routine, the reason for referral may be detection of disease not only in the bones but also non-osseous metastases. In this regard PSMA-PET/CT and WB-MRI have an advantage owing to their potential to assess osseous and non-osseous lesions in a single examination. NaF-PET performed with a diagnostic CT scan is an alternative "one stop shop" examination as enlarged lymph nodes and soft tissue metastases can be detected by the contrast-enhanced CT scan. Furthermore, the latest hybrid imaging method PET/MRI has the advantage of a reduced radiation dose compared to PET/CT, but the future role of PET/MRI is not yet established.

This study has limitations. First, it is based on a selected group of patients representing a broad disease spectrum. Second, a limited number of study participants were included in this study. Despite the limited statistical power, a significant difference between the overall accuracy of PSMA-PET/CT

compared to WB-MRI was found. Third, the WB-MRI protocols did not meet the recently introduced MET-RADS-P criteria as the data collection was initiated before this publication came out [40]. Neither Dixon techniques with subsequent reconstruction of fat images nor sagittal spine STIR were included in the present study. The use of MET-RADS-P protocols for WB-MRI might improve the diagnostic performance of WB-MRI in the future. Fourth, a histological reference standard would have been preferable in this study. However, biopsies of involved and non-involved bones were neither practically nor ethically possible. Encouragingly, previous studies have reported that accumulated ^{68}Ga-PSMA correlates to a high degree with histologically verified prostate cancer cells in the prostate and lymph nodes [41–43]. A panel diagnosis based on multiple sources of information has been described as a plausible method to evaluate diagnostic tests when there is no gold standard and constituted the final diagnosis in this study as in numerous previous studies [22, 28, 29, 44, 45]. In patients with a concordant diagnosis of PSMA-PET/CT, NaF-PET/CT and WB-MRI, this conclusion constituted the final diagnosis, and a similar approach has been described in previous studies [41–43]. Evidence seemed solid with three teams of readers reaching the same diagnosis based on imaging methods visualising three different entities of bone metastases (PSMA expression, bone remodelling, restricted water diffusion). However, a final diagnosis based on the index tests investigated can lead to an incorporation bias and a possible overestimation of the diagnostic performances, but might not privilege one or the other of the imaging techniques investigated [28].

This study aimed to add to the sparse prospective literature on the diagnostic accuracy of PSMA-PET/CT for the detection of bone metastases and to perform a comparison with NaF-PET/CT and WB-MRI. In conclusion, the results indicate that PSMA-PET/CT has a superior diagnostic performance compared to WB-MRI, but not to NaF-PET/CT. However, further prospective diagnostic accuracy studies including recently introduced WB-MRI protocols are required

to confirm these results and investigate whether PSMA-PET/CT can outperform NaF-PET/CT in a larger sample. PSMA-PET/CT has potential as a "one stop shop" examination evaluating bone as well as soft tissue metastases and the option of $^{177}$Lu PSMA treatment. With the possible substitution of $^{68}$Ga-PSMA with $^{18}$F-PSMA, the use of PSMA-PET/CT might be feasible, but the use will ultimately depend on priorities in local health care systems and reimbursement policies.

## Compliance with ethical standards

**Guarantor** The scientific guarantor of this publication is Eva Dyrberg.

**Conflict of interest** The authors of this manuscript declare no relationships with any companies whose products or services may be related to the subject matter of the article.

**Statistics and biometry** Tobias W. Klausen and Stig S. Mortensen kindly provided statistical advice for this manuscript.

**Informed consent** Written informed consent was obtained from all subjects (patients) in this study.

**Ethical approval** Institutional review board approval was obtained.

**Methodology**
• prospective
• diagnostic study
• performed at one institution

## References

1. Herrera FG, Tawadros T, Berthold DR (2015) Bone cancer. Primary bone cancers and metastases, 2nd edn. Elsevier, San Diego
2. Thurairaja R, Mcfarlane J, Traill Z, Persad R (2004) State-of-the-art approaches to detecting early bone metastatic spread and changes to bone biology in prostate cancer. BJU Int 94:268–271
3. Moulopoulos LA, Koutoulidis V (2015) Bone marrow MRI, 1st edn. Springer-Verlag Italia, Milan
4. Kingsley LA, Fournier PGJ, Chirgwin JM, Guise TA (2007) Molecular biology of bone metastasis. Mol Cancer Ther 6:2609–2617
5. Elgazaar A (2006) The pathophysiologic basis of nuclear medicine, 2nd edn. Springer, Berlin Heidelberg
6. Høilund-Carlsen PF, Hess S, Alavi A (2017) Bone marrow and NOT bone metastases is what 21st century diagnostic imaging must focus upon when looking for skeletal metastases. J Nucl Med. https://doi.org/10.2967/jnumed.117.201848
7. Mottet N, Bellmunt J, Bolla M et al (2017) EAU-ESTRO-SIOG guidelines on prostate cancer. Part 1: screening, diagnosis, and local treatment with curative intent. Eur Urol 71:618–629
8. Mohler JL, Armstrong AJ, Bahnson RR et al (2016) Prostate cancer, version 1.2016. J Natl Compr Canc Netw 14:19–30
9. Fogelman I, Blake GM, Cook GJR (2013) The isotope bone scan: we can do better. Eur J Nucl Med Mol Imaging 40:1139–1140
10. Gillessen S, Attard G, Beer TM et al (2018) Management of patients with advanced prostate cancer: the report of the advanced prostate cancer consensus conference APCCC 2017. Eur Urol 73:178–211
11. Bertoldo F, Boccardo F, Bombardieri E et al (2017) Bone metastases from prostate cancer, 1st edn. Springer, Cham
12. Eiber M, Fendler WP, Rowe SP et al (2017) Prostate-specific membrane antigen ligands for imaging and therapy. J Nucl Med 58:67S–76S
13. Hofman MS, Hicks RJ, Maurer T, Eiber M (2018) Prostate-specific membrane antigen PET: clinical utility in prostate cancer, normal patterns, pearls, and pitfalls. Radiographics 38:200–217
14. Silver DA, Pellicer I, Fair WR, Heston WD, Cordon-Cardo C (1997) Prostate-specific membrane antigen expression in normal and malignant human tissues. Clin Cancer Res 3:81–85
15. Evangelista L, Briganti A, Fanti S et al (2016) New clinical indications for (18)F/(11)C-choline, new tracers for positron emission tomography and a promising hybrid device for prostate cancer staging: a systematic review of the literature. Eur Urol 70:161–175
16. Zacho HD, Nielsen JB, Haberkorn U, Stenholt L, Petersen LJ (2017) $^{68}$Ga-PSMA PET/CT for the detection of bone metastases in prostate cancer: a systematic review of the published literature. Clin Physiol Funct Imaging. https://doi.org/10.1111/cpf.12480
17. Tateishi U, Morita S, Taguri M et al (2010) A meta-analysis of (18)F-fluoride positron emission tomography for assessment of metastatic bone tumor. Ann Nucl Med 24:523–531
18. Pasoglou V, Michoux N, Larbi A, Van Nieuwenhove S, Lecouvet F (2018) Whole body MRI and oncology: recent major advances. Br J Radiol. https://doi.org/10.1259/bjr.20170664%0A
19. Tombal B, Lecouvet F (2012) Modern detection of prostate cancer's bone metastasis: is the bone scan era over? Adv Urol. https://doi.org/10.1155/2012/893193
20. Padhani AR, Koh D-M, Collins DJ (2011) Whole-body diffusion-weighted MR imaging in cancer: current status and research directions. Radiology 261:700–718
21. Bossuyt PM, Reitsma JB, Bruns DE et al (2015) STARD 2015: an updated list of essential items for reporting diagnostic accuracy studies. Radiology 277:826–832
22. Lecouvet FE, El Mouedden J, Collette L et al (2012) Can whole-body magnetic resonance imaging with diffusion-weighted imaging replace Tc 99m bone scanning and computed tomography for single-step detection of metastases in patients with high-risk prostate cancer? Eur Urol 62:68–75
23. Afshar-Oromieh A, Zechmann CM, Malcher A et al (2014) Comparison of PET imaging with a (68)Ga-labelled PSMA ligand and (18)F-choline-based PET/CT for the diagnosis of recurrent prostate cancer. Eur J Nucl Med Mol Imaging 41:887–897
24. Afshar-Oromieh A, Avtzi E, Giesel FL et al (2015) The diagnostic value of PET/CT imaging with the (68)Ga-labelled PSMA ligand HBED-CC in the diagnosis of recurrent prostate cancer. Eur J Nucl Med Mol Imaging 42:197–209
25. Morigi JJ, Stricker P, Van Leeuwen P et al (2015) Prospective comparison of the detection rate of 18F-fluoromethylcholine and 68Ga-PSMA-HBED PET/CT in men with prostate cancer with rising PSA post curative treatment, being considered for targeted therapy. J Nucl Med 56:1185–1191
26. Ceci F, Uprimny C, Nilica B et al (2015) (68)Ga-PSMA PET/CT for restaging recurrent prostate cancer: which factors are associated with PET/CT detection rate? Eur J Nucl Med Mol Imaging 42:1284–1294
27. Eiber M, Maurer T, Souvatzoglou M et al (2015) Evaluation of hybrid 68Ga-PSMA ligand PET/CT in 248 patients with biochemical recurrence after radical prostatectomy. J Nucl Med 56:668–674
28. Pyka T, Okamoto S, Dahlbender M et al (2016) Comparison of bone scintigraphy and $^{68}$Ga-PSMA PET for skeletal staging in prostate cancer. Eur J Nucl Med Mol Imaging 43:2114–2121

29. Janssen J, Meißner S, Woythal N et al (2018) Comparison of hybrid 68Ga-PSMA-PET/CT and 99mTc-DPD-SPECT/CT for the detection of bone metastases in prostate cancer patients: additional value of morphologic information from low dose CT. Eur Radiol 28:610–619

30. Evangelista L, Bertoldo F, Boccardo F et al (2016) Diagnostic imaging to detect and evaluate response to therapy in bone metastases from prostate cancer: current modalities and new horizons. Eur J Nucl Med Mol Imaging 43:1546–1562

31. Woo S, Suh CH, Kim SY et al (2018) Diagnostic performance of magnetic resonance imaging for the detection of bone metastasis in prostate cancer: a systematic review and meta-analysis. Eur Urol 73:81–91

32. Wondergem M, van der Zant FM, van der Ploeg T, Knol RJJ (2013) A literature review of 18F-fluoride PET/CT and 18F-choline or 11C-choline PET/CT for detection of bone metastases in patients with prostate cancer. Nucl Med Commun 34:935–945

33. Luzzati A, Scotto G, Perrucchini G, Zoccali C (2017) Surgery: treatment of oligometastatic disease. In: Bertoldo F, Boccardo F, Bombardieri E et al (eds) Bone metastases from prostate cancer, 1st edn. Springer, Cham, pp 147–161

34. Avuzzi B, Valdagni R (2017) Bone metastases from prostate cancer: radiotherapy. In: Bertoldo F, Boccardo F, Bombardieri E et al (eds) Bone metastases from prostate cancer, 1st edn. Springer, Cham, pp 163–180

35. Fendler WP, Calais J, Allen-Auerbach M et al (2017) ^{68}Ga-PSMA-11 PET/CT interobserver agreement for prostate cancer assessments: an international multicenter prospective study. J Nucl Med 58:1617–1623

36. Mannweiler S, Amersdorfer P, Trajanoski S et al (2009) Heterogeneity of prostate-specific membrane antigen (PSMA) expression in prostate carcinoma with distant metastasis. Pathol Oncol Res 15:167–172

37. Fendler WP, Eiber M, Beheshti M et al (2017) ^{68}Ga-PSMA PET/CT: joint EANM and SNMMI procedure guideline for prostate cancer imaging: version 1.0. Eur J Nucl Med Mol Imaging 44:1014–1024

38. Giesel FL, Hadaschik B, Cardinale J et al (2017) F-18 labelled PSMA-1007: biodistribution, radiation dosimetry and histopathological validation of tumor lesions in prostate cancer patients. Eur J Nucl Med Mol Imaging 44:678–688

39. Ceci F, Castellucci P, Cerci JJ, Fanti S (2017) New aspects of molecular imaging in prostate cancer. Methods 130:36–41

40. Padhani AR, Lecouvet FE, Tunariu N et al (2017) METastasis reporting and data system for prostate cancer: practical guidelines for acquisition, interpretation, and reporting of whole-body magnetic resonance imaging-based evaluations of multiorgan involvement in advanced prostate cancer. Eur Urol 71:81–92

41. Beheshti M, Vali R, Waldenberger P et al (2008) Detection of bone metastases in patients with prostate cancer by 18F fluorocholine and 18F fluoride PET-CT: a comparative study. Eur J Nucl Med Mol Imaging 35:1766–1774

42. McCarthy M, Siew T, Campbell A et al (2011) ^{18}F-Fluoromethylcholine (FCH) PET imaging in patients with castration-resistant prostate cancer: prospective comparison with standard imaging. Eur J Nucl Med Mol Imaging 38:14–22

43. Garcia JR, Moreno C, Valls E et al (2015) Diagnostic performance of bone scintigraphy and 11C-choline PET/CT in the detection of bone metastases in patients with biochemical recurrence of prostate cancer. Rev Esp Med Nucl Imagen Mol 34:155–161

44. Fonager RF, Zacho HD, Langkilde NC et al (2017) Diagnostic test accuracy study of 18F-sodium fluoride PET/CT, 99mTc-labelled diphosphonate SPECT/CT, and planar bone scintigraphy for diagnosis of bone metastases in newly diagnosed, high-risk prostate cancer. Am J Nucl Med Mol Imaging 7:218–227

45. Jambor I, Kuisma A, Ramadan S et al (2016) Prospective evaluation of planar bone scintigraphy, SPECT, SPECT/CT, 18F-NaF PET/CT and whole body 1.5T MRI, including DWI, for the detection of bone metastases in high risk breast and prostate cancer patients: SKELETA clinical trial. Acta Oncol 55:59–67